

Power Regulation in High Performance Multicore Processors[†]

X. Chen, Y. Wardi, and S. Yalamanchili*

Abstract—This paper presents, implements, and evaluates a power-regulation technique for multicore processors, based on an integral controller with adjustable gain. The gain is designed for wide stability margins, and computed in real time as part of the control law. The tracking performance of the control system is robust with respect to modeling uncertainties and computational errors in the loop. The main challenge of designing such a controller is that the power dissipation of program-workloads varies widely and often cannot be measured accurately; hence extant controllers are either ad hoc or based on a-priori modeling characterizations of the processor and workloads. Our approach is different. Leveraging the aforementioned robustness it uses a simple textbook modeling framework, and adjusts its parameters in real time by a system-identification module. In this it trades modeling precision for fast computations in the loop making it suitable for on-line implementation in commodity data-center processors. Consequently, the proposed controller is agnostic in the sense that it does not require any a-priori system characterizations. We present an implementation of the controller on Intel’s fourth-generation microarchitecture, Haswell, and test it on a number of industry benchmark programs which are used in scientific computing and datacenter applications. Results of these experiments are presented in detail exposing the practical challenges of implementing provably-convergent power regulation solutions in commodity multicore processors.

I. INTRODUCTION

For decades, scaling of transistors to decreasing geometries was the primary source of increased processor performance. This was accompanied by the corresponding scaling of device power thereby keeping power densities roughly constant on a processor die. However, this behavior known as Dennard scaling has ended leading to unsustainable growth in power consumption in future processors as we increase the number of transistors on a die. Therefore, to continue to sustain performance scaling we must seek new and innovative advances in power management in multicore processors. Such advances are central to the effective operation of all modern processors in platforms ranging from mobile devices to data centers and high-performance computing (HPC) machines that drive national initiatives in key areas such as science, finance, and defense [1], [2].

In multicore processors, the relationships between workloads, power dissipation, resulting thermal fields, and their interaction with the leakage current present new and unresolved power and thermal management challenges. For example, application workloads exhibit time-varying computation and memory access behaviors resulting in spatially

and temporally varying power dissipation and non-uniform thermal fields. The cross-chip variations in temperature couples to circuit leakage and delay, increases full-chip leakage power, reduces peak throughput, degrades chip/package reliability, and increases cooling/package costs. Thus, effective control of power dissipation is critical to the reliable and high performance operation of multicore processors. This paper describes a novel and effective power regulation technique and the results of an evaluation of its implementation on a commodity multicore processor.

Modern multicore processors are organized into several *voltage islands* where each island may comprise of one or more processing cores. Each voltage island can operate at one of several discrete *power states* each defined by an operational voltage-frequency pair. A general technique for controlling power and temperature is based on setting the appropriate power state of each voltage island. This is commonly referred to as Dynamic Voltage/Frequency Scaling, or DVFS. The development of effective controls based on DVFS faces several challenges. First, the relationship between the clock frequency and core power is complicated by other factors such as the coupling between temperature and leakage power. Second, application workloads have time-varying compute and memory system behaviors requiring a robust, adaptive control strategy to manage power dissipation. Third, distinct cores in a voltage island execute distinct instruction streams with distinct behaviors but may share a common clock and hence frequency. For example, the Intel Haswell processor tested in this paper has four cores sharing a single voltage island and executing eight hardware threads (subprograms) at the same frequency [3].

A number of DVFS heuristics have been proposed to control power dissipation. Prominent are heuristics for clock gating [4], thread migration [5][6], prediction [7] and voltage scaling [8]. However, heuristics are limited in their scope and robustness. Consequently, several efforts have applied feedback control theory as an effective way to improve performance and robustness [9], [10], [11]. Generally, such controllers relied on off-line analysis of anticipated workloads [10], [1] or empirical approaches [12], [13] to derive control parameters. This includes efforts to limit operation below a maximum power constraint [14], [15]. However, all of these approaches are applied to applications that have been profiled a priori to derive the control parameters.

This paper concerns a control law that is not based on any off-line profiling (hence said to be *agnostic*), and it estimates the model-parameters on line by least-square system identification. The control law is comprised of a standalone integrator with adaptive gain. Now it is well-known that an

[†]Research supported in part by the NSF under Grant CNS-1239225.

*School of Electrical and Computer Engineering, Georgia Institute of Technology, Atlanta, GA 30332. Email: xchen318@gatech.edu, ywardi@ece.gatech.edu, sudha@ece.gatech.edu.

integral control can have poor stability margins and oscillations in the system's response, hence it is often supplemented by proportional and derivative elements in order to form the PID control [16]. We use a different approach, consisting of a standalone integrator with a variable gain, designed for fast convergence, wide stability margins, and reduced oscillations as compared to fixed-gain integrators. Moreover, its tracking performance and stability are quite robust to modeling variations and computing errors in the loop, and hence we need not worry about precise model parameters. Furthermore, we can speed up the computations in the loop at the expense of precision if needed.¹

The controller described in the sequel was first designed for regulating the dynamic power in computer cores in Ref. [17]. Subsequently it has been analyzed in an abstract setting in [18], where its convergence, stability, and robustness were proved. Its performance was tested via simulation on instruction-throughput regulation [19], [20], then on throughput of abstract Discrete Event Dynamic Systems (DEDS) such as queues, Petri nets and transportation networks [21]. Lately the controller has been implemented on Intel's fourth-generation micro-architecture, Haswell [22], where it was tested on instruction-throughput regulation.

This paper concerns an implementation of the controller on a Haswell machine and evaluations of its application to power regulation. It makes the following specific contributions: 1). It is the first to present an implementation of an integral control for power regulation in multicore processors. 2). It is agnostic, and adjusts well to workload variations. 3). It is the first (to our knowledge) to use on-line system identification for estimating a suitable system-model. 4). It is applied to timely data-center applications. 5). It converges quite fast.

The rest of the paper is organized as follows. Section II describes the problem, system-model, and power-regulation technique, and recounts established results. Section III presents test results of applications of the controller to industry-benchmarks, and Section IV concludes the paper.

II. POWER REGULATION TECHNIQUE

This section first describes the regulation technique in the abstract setting considered in [18] in order to highlight its general salient features. Then it discusses its particular applications to power control in multicore processors.

Consider the single-input-single-output discrete-time system shown in Figure 1, where $k = 1, 2, \dots$ represents discrete time, $r \in R$ is a reference input, $y_k \in R$ is the output, u_k is the control variable, and $e_k \in R$ is the error signal. Generally the plant can be nonlinear and time varying, and the objective of the controller is to have the output y_k , $k = 1, 2, \dots$, track the reference r .

¹Refs. [17], [18] argue for the choice of the variable-gain integral control described in this paper over a PID controller, based on its robustness and flexibility in implementation. Furthermore, we have tested via simulation (not reported here) the addition of a proportional element to the integral controller but found no improvement.

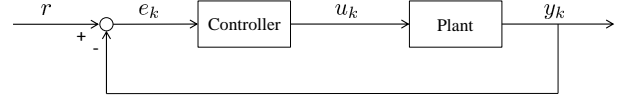


Fig. 1: Closed Loop Control System

The controller we choose has the form

$$u_k = u_{k-1} + A_k e_{k-1}, \quad i = 1, 2, \dots, \quad (1)$$

where A_k is the gain at time k , assumed to be positive. If $A_k = A$ where $A > 0$ does not depend on time k then we recognize the controller as an adder, a discrete-time equivalent of an integrator. Since generally A_k depends on k , we call the controller a *variable-gain integrator*. The plant generally characterizes the relationship between the control signal $\{u_k\}$ and the output process $\{y_k\}$. Of a particular interest to us is the partial derivative $\frac{\partial y_{k-1}}{\partial u_{k-1}}$, which we assume to be nonzero. For reasons that will become apparent shortly, we would like to set the controller's gain to $A_k = \left(\frac{\partial y_{k-1}}{\partial u_{k-1}}\right)^{-1}$. In this we assume that the partial derivative $\frac{\partial y_{k-1}}{\partial u_{k-1}}$ is computable in real time from suitable measurements of the system, and hence can play a part in the control law. However, such real-time computations may be subjected to delays and errors. Therefore an approximation may have to be used, resulting in the following definition of the controller's gain,

$$A_k = \frac{1}{\frac{\partial y_{k-1}}{\partial u_{k-1}} + \eta_{k-1}}, \quad (2)$$

where η_{k-1} denotes an additive error. To complete the characterization of the loop we note that the tracking error is

$$e_k = r - y_k \quad (3)$$

as is evident from Figure 1. The control law consists of repeated recursive applications of Equations (2)-(1)-(3).

The rationale behind the choice of A_k in Eq. (2) can be seen by considering for a moment the case where the plant is a memoryless nonlinearity, hence described by the relation $y_k = g(u_k)$ for a differentiable function $g: R \rightarrow R$. In this case $\frac{\partial y_{k-1}}{\partial u_{k-1}} = \frac{dg}{du}(u_{k-1})$, and Eqs. (1) - (3) result in

$$u_k = u_{k-1} + \frac{1}{\frac{dg}{du}(u_{k-1}) + \eta_{k-1}} (r - g(u_{k-1})). \quad (4)$$

We recognize this as the Newton-Raphson method for solving the equation $r - g(u) = 0$, where the derivative term $\frac{dg}{du}(u_{k-1})$ is corrupted by the additive error η_{k-1} . There are well-known convergence results including a geometric convergence rate, namely the existence of $\theta < 1$ such that

$$|r - g(u_k)| < \theta |r - g(u_{k-1})|, \quad k = 1, 2, \dots; \quad (5)$$

see [23]. In particular, Equation (5) holds under substantial upper bounds on the relative error $\mathcal{E}_{k-1} := |\eta_{k-1}| / \left|\frac{dg}{du}(u_{k-1})\right|$, hence convergence of the Newton-Raphson method is said to be robust with respect to errors in the derivative $\frac{dg}{du}(u_{k-1})$.

These results have been extended to the more-general setting where the plant-system is dynamic (as opposed to memoryless), stochastic and time-varying. In such setting the term $\frac{dg}{du}(u_{k-1})$ makes no sense but the term $\frac{\partial y_{k-1}}{\partial u_{k-1}}$ in Eq. (2) can be well defined. One cannot expect convergence in the form of the limit $\lim_{k \rightarrow \infty} (r - y_k) = 0$ to hold true due to variations in the system's characteristics. However, results of the form $\limsup_{k \rightarrow \infty} |r - y_k| < \varepsilon$ were obtained in [18] for a suitable $\varepsilon > 0$ which depends on a measure of the system's variability. The geometric convergence expressed in Eq. (5) is extended as long as $|r - y_k|$ is not too small, even for fairly large errors $|\eta_{k-1}|$. These last two results imply fast approach of the tracking algorithm towards its target r (though not its convergence exactly to r), and its robustness with respect to computational errors of the derivative term $\frac{\partial y_{k-1}}{\partial u_{k-1}}$.

In the context of computer processors, this technique was applied to regulate instructions' throughput. The plant is modelled as a discrete event dynamic system controlled by the processor's clock rate (frequency), whose output is the average instruction-throughput measured over short time frames. The technique was verified by both simulation [19], [20] and implementation on a Haswell machine [22]. In simulation the derivative term $\frac{\partial y_{k-1}}{\partial u_{k-1}}$ is estimated by Infinitesimal Perturbation Analysis [24], [25], and in implementation a cruder but faster approximation is used. This paper concerns power regulation which poses a different set of challenges, and it uses a system characterization as described in the following paragraphs.

The power dissipated in a core has two major components, static power and dynamic power, respectively denoted by P_s and P_d ; Thus

$$P = P_s + P_d. \quad (6)$$

The dynamic power is due to the switching activities at the gates of the core. It depends on the supply voltage V , clock rate (frequency) ϕ , core's capacitance C , and the program-workload α representing the switching activities in the core's transistor gates. This dependence is represented by the equation

$$P_d = \alpha C V^2 \phi; \quad (7)$$

see [26]. Generally C is a constant which can be assessed empirically, but $\alpha = \alpha(t)$ varies rapidly with the program load and cannot be measured. The relationship between frequency and voltage often is affine, namely $V = a + m\phi$. In this case, and in light of Eq. (7), P_d can be expressed as a third-degree polynomial in ϕ . However, it may be impossible to empirically determine the coefficients of this polynomial due to rapid variations of $\alpha(t)$. Furthermore, often it is impossible to measure the dynamic power but only the total power P . Consequently we are unable to compute the coefficients of the polynomial function relating frequency to dynamic power. As a matter of fact, earlier attempt to apply the regulation algorithm on Haswell with various fixed polynomial coefficients determined off line failed to yield the desired tracking.

The static power depends on the supply voltage and temperature, while the temperature depends on the total power (see [26]). This circular relationship between power and temperature precludes the existence of a simple model relating frequency to static power. Moreover, the temperature may vary during program execution, further complicating the prospects of a frequency-to-power tractable model that can be used in a real-time control.

As mentioned in the introduction, the Haswell machine which serves as the implementation platform consists of four cores processing eight concurrent threads. All of the cores reside in the same voltage island, hence we cannot control each one of them separately but rather control them jointly by a common frequency, the *processor frequency*. The controlled quantity is the average power among the four cores, called the *processor power*. In the setting of Figure 1, we partition the time horizon into equally-spaced contiguous intervals called *control cycles* and denoted by $C_k, k = 1, 2, \dots$; u_k is the processor frequency applied during C_k , and y_k is the average among the cores of the mean spatial and temporal power measured during C_k at each core. A key question is how to obtain an estimate of the derivative term $\frac{\partial y_{k-1}}{\partial u_{k-1}}$, in Equation (2). This requires knowledge of some parameters of the plant model relating u_k to y_k , but such a model is only partly available. In fact, we mentioned that there is no analytic model for the static power, and while there is an adequate third-degree polynomial for the dynamic power, its coefficients change with time at a high rate.

We overcome these problems by the following approach. First, we search for a third-order polynomial for estimating the relation between the applied frequency and the total processor power. This of course can fit the dynamic power but not the static power. However, in computing applications at the frequency range considered in this paper, the static power comprises 20% - 30% of the total power, and therefore we feel confident leveraging the aforementioned robustness of the performance of the tracking controller with respect to errors in computing $\frac{\partial y_{k-1}}{\partial u_{k-1}}$. Second, to cope with the rapid variations in the coefficients of this polynomial due to changes in $\alpha(t)$, we use a system identification module run concurrently, in real time, along the program-executions by the processor.

Let us denote by $p_k(\phi) := a_k \phi^3 + b_k \phi^2 + c_k \phi + d_k$ the estimator polynomial during C_k , then its derivative $\frac{dp_{k-1}}{d\phi}(\phi_{k-1}) = 3a_{k-1} \phi_{k-1}^2 + 2b_{k-1} \phi_{k-1} + c_{k-1}$ is the term $\frac{\partial y_{k-1}}{\partial u_{k-1}} + \eta_{k-1}$ in Equation (2). A system identification module, comprised of a standard recursive least-square estimator (e.g., [27]), is used to compute the coefficient-vector $x_k := (a_k, b_k, c_k, d_k)$ during C_{k-1} .

It must be pointed out that performance of the power regulator is affected by several practical considerations. First, the rate at which energy and power can be measured is determined by the processor vendor, which in this case is Intel. The model specific registers are updated at approximately 1 ms intervals but no timestamp is provided so it is not possible to know when the measurement interval began.

Consequently, mapping measurements to application code is difficult and can cause larger deviations in regulated power than the model would otherwise achieve. Second, the current manner in which the frequency is changed is via file I/O incurring substantial latency relative to the execution time of instructions. If program behavior changes significantly during this interval, tracking becomes more challenging. For example, data center programs that possess poor spatial and temporal reference locality and are memory intensive will exhibit wide variations in average instruction execution time due to memory accesses. High latency in setting the processor frequency will make it difficult to rapidly adapt to changes in power consumption and consequently will affect the rate of convergence of the power regulator and the choice of the duration of the control cycle. Such practical considerations must be overcome by robustness in the design of the regulator.

III. RESULTS

The proposed power regulator was tested on various programs from two suites of industry benchmarks, Splash 2 and GraphBig. Splash 2 is a set of standard benchmark programs for shared memory cache coherent multiprocessors [28]. It includes a collection of multithreaded workloads representing traditional engineering and science applications. The majority of the benchmarks are from the traditional high performance computing domain while several are drawn from signal processing and general engineering computations such as computer graphics. GraphBIG is a set of benchmark programs that perform computations over graphs [29], and was inspired by the IBM System G project, surveyed in the sequel.

We are witnessing an explosive growth in modern data science applications executing in data centers that deal with data that is of the relational form and can be represented by graph data structures with large numbers of node and edge properties. These applications have irregular memory access patterns, exhibit low spatial and temporal locality, and are characterized by low operation density, i.e., number of operations per byte of data accessed. Consequently, they stress the memory system and challenge optimizations for achieving high processor utilization. To cover major graph computation types and data sources encountered in such data center applications, GraphBIG incorporates representative data structures, workloads and data sets from 21 real-world use cases from multiple application domains. As a complement to traditional science and engineering applications represented by the Splash-2 benchmarks, GraphBIG represents the relational computation driving commercial sectors such as retail forecasting, data analytics, finance, and banking.

We implemented the controller by loading a C++ program to the Haswell processor via the

PAPI interface [30].² The Haswell processor has a finite set of 16 frequencies, namely $\Omega := \{0.8, 1.0, 1.1, 1.3, 1.5, 1.7, 1.8, 2.0, 2.2, 2.4, 2.5, 2.7, 2.9, 3.1, 3.2, 3.4\}$ in GHz. Therefore, we augmented Eq. (1) by projecting its Reft-Hand Side (RHS) onto Ω . That is, with $P_{\Omega}(u) := \operatorname{argmin}\{|v - u| : v \in \Omega\}$ for $u \in R$ (with $v < u$ if the argmin is not unique), we replace (1) by the following equation,

$$u_k = P_{\Omega}(u_{k-1} + A_k e_{k-1}). \quad (8)$$

The control algorithm consists of a recursive application of Eqs. (2)-(8)-(3).

The control cycles of the algorithm can be chosen according to performance considerations such as settling times, subject to hardware constraints. At the end of each control cycle, first the model parameters are recomputed by the system identification module and then the operating frequency is assigned to the processor for the next period. In the Haswell processor that we use, energy consumption values are provided at a sampling interval of 1 ms. Hence we pick control cycles that are multiples of this interval.³ We test the control algorithm at two different rates associated with the control cycles of 10 ms and 30 ms, and we depict graphs of power as function of time during the first 4,000 ms of program executions.

A. Splash-2 benchmark programs

We tested the controller on two programs: *Barnes*, and *Ocean-nc*. Barnes is a compute intensive application with under 10% of memory-access instructions. In contrast, Ocean-nc is a memory-intensive program with memory-bound instructions in the 30% – 50% range for typical applications. In both cases we set the power-target value to 10 W.

Consider first Barnes. For control cycles of 10 ms, results of an application of the control algorithm are shown in Figure 2 and Figure 3. Figure 2 depicts the graph of power vs. time for the first 4,000 ms, corresponding to 400 iterations. The power rises from an initial value of 6.34 W, and following a period of transient behavior lasting 720 ms, taking 72 control cycles, it settles into an oscillatory behavior about the target value of 10 W. The average power computed over the interval [720, 4000] ms (after the power has settled for the first time into an oscillation about the target level) is 10.2604 W, which is 0.2604 W above the target level of 10 W.

The graph of the frequency (clock rate) vs. time is shown in Figure 3. The larger oscillations in the first 1,400 ms likely are due to the fact that early in the program there are more memory instructions than in the last 2,600 ms. Memory instructions can take one-to-two orders more time than computational instructions. Therefore memory-intensive

²Modern microprocessors include hardware counters that record the occurrences of various events during program executions, like completion of instructions' executions, cache misses, etc. The Performance Application Programming Interface (PAPI) is a publicly available software infrastructure for accessing these performance counters during program execution.

³The power measurements are indirect. Haswell provides an energy counter, so we can measure the energy in 1 ms and divide the result by the measurement time to obtain the average power during 1 ms periods.

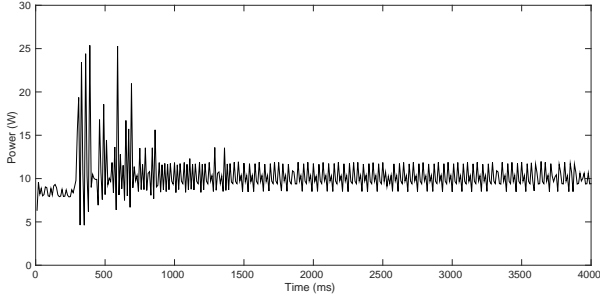


Fig. 2: Barnes: power vs. time, control cycle = 10 ms

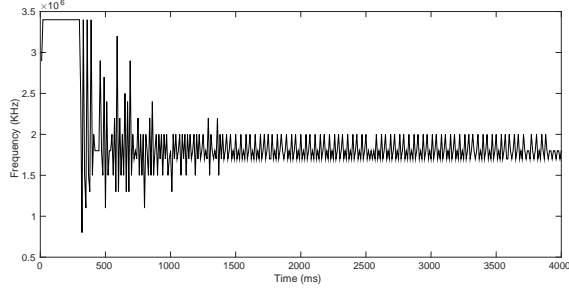


Fig. 3: Barnes: clock frequency vs. time, control cycle = 10 ms

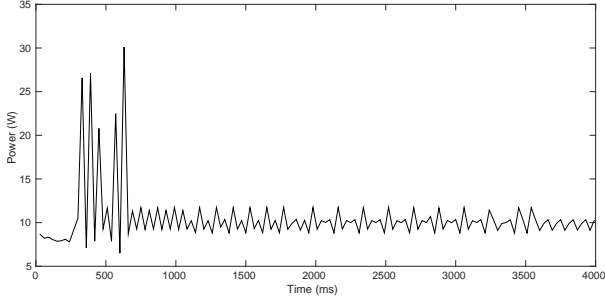


Fig. 4: Barnes: power vs. time, control cycle = 30 ms

periods tend to have greater variability in the program workload and hence larger changes in frequency and power. The persistence of the smaller oscillations throughout the interval $[1400, 4000]$ ms likely is due to quantization effects associated with the fact that the frequency-set Ω is finite. The average frequency in the interval $[720 - 4000]$ ms is 1.93 GHz.

For the control cycle of 30 ms, the graph of power vs. time is depicted in in Figure 4. The power rises from an initial value of 8.6543 W, and after 720 ms (or 24 control cycles) it settles around the target value of 10 W. Its average in the interval $[720, 4000]$ ms is 10.4344 W, which is 0.4344 W over the target level of 10 W. The frequency profile is similar to that of Figure 3 and hence not shown, and its average in the interval $[720, 4000]$ ms is 1.89 GHz.

Table I summarizes the time it takes the power to settle about its target value for the first time, as well as the absolute value of the error (difference) between the average power and the target value of 10 W. The performance of the controller is similar for the two control cycles, and the indicated minor

TABLE I: Barnes: power error and settling time

| Control Cycle (ms) | 10 | 30 |
|--------------------|--------|--------|
| Error (W) | 0.2604 | 0.4344 |
| Settling Time (ms) | 720 | 720 |

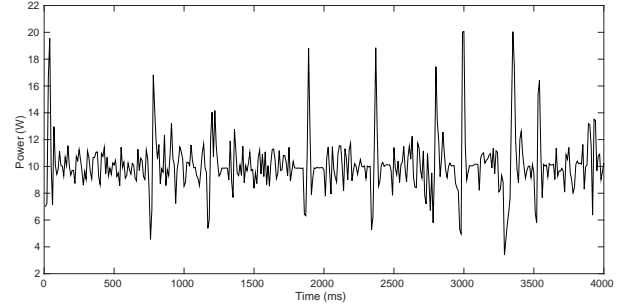


Fig. 5: Ocean-nc: power vs. time, control cycle = 10 ms

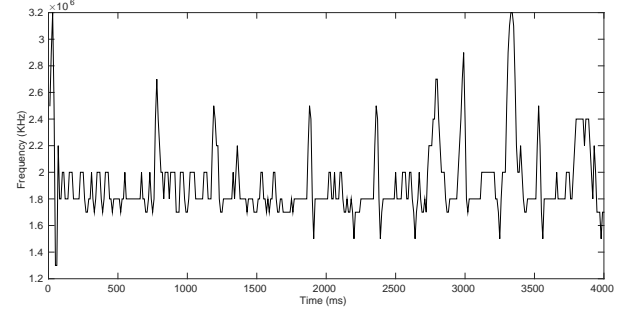


Fig. 6: Ocean-nc: clock frequency vs. time, control cycle = 10 ms

differences likely are due to the frequency quantization.

Consider next Ocean-nc. Graphs of power and frequency vs. time are depicted in Figure 5 and Figure 6, respectively. The power rises from an initial value of 7.015 W, and following a period of transient behavior lasting 1,240 ms, taking 124 control cycles, it settles into an oscillatory behavior about the target value of 10 W. The average power computed over the interval $[1240, 4000]$ ms is 10.1269 W, which is 0.1269 W above the target level of 10 W. The average frequency is 1.918 GHz.

For 30 ms-control cycles, the graph of power vs. time is depicted in in Figure 7 while the frequency graph displays similar characteristics to that in Figure 6 for 10 ms-control cycles, hence not shown. The power rises from an initial value of 5.483 W, and after 1,710 ms (or 57 control cycles) it settles around the target value of 10 W. Its average in the interval $[1710, 4000]$ ms is 9.9298 W, which is 0.0702 W below the target level of 10 W. The average frequency is 1.86 GHz. The results are summarized in Table II. A comparison between the results for Barnes and Ocean-nc will be made in Subsection III.C, below.

B. GraphBig benchmark experiments

We tested the controller on two GraphBig programs: *Breadth-first Search (BFS)*, and *Kcore*. BFS is one of the most fundamental operations of graph computing, while kCore encompasses topological analysis of graphs and is

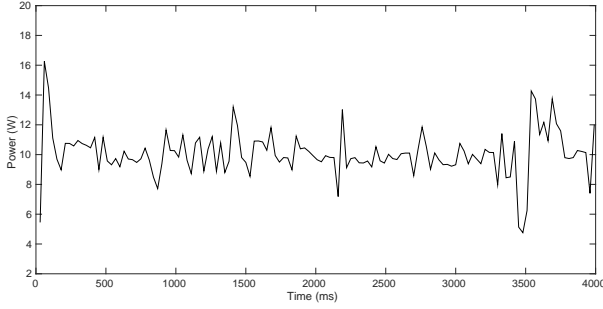


Fig. 7: Ocean-nc: power vs. time, control cycle = 30 ms

TABLE II: Ocean-nc: power error and settling time

| Control Cycle (ms) | 10 | 30 |
|--------------------|--------|--------|
| Error (W) | 0.1269 | 0.0702 |
| Settling Time (ms) | 1240 | 1710 |

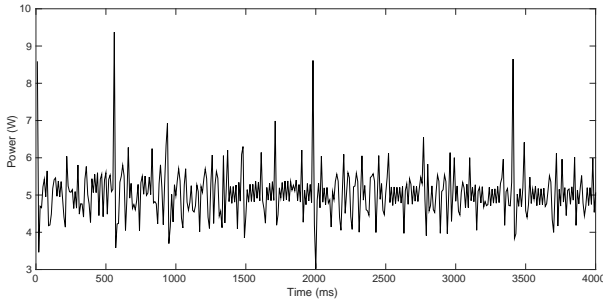


Fig. 8: BFS: power vs. time, control cycle = 10 ms

representative of approaches to the structural analysis of graphs. Both programs represent large-scale computations executed over clusters of servers in large data centers.

For both BFS and Kcore the target power is 5 W. The reason it is less that the target for the Splash-2 programs (10 W) is that a GraphBig program typically has a higher fraction of memory-access instructions than Splash-2 programs, which tend to be low-frequency, low-power operations.

Consider first the BFS program. For 10 ms-control cycles, the results are shown in Figure 8 and Figure 9. The power vs. time graph is depicted in Figure 8. The power starts at the initial value of 8.57 W, and following an initial transient lasting 380 ms (or 38 control cycles) it settles about the target value of 5 W. The average power in the interval [380,4000] ms is 5.0542 W, which is 0.0542 W more than the target level of 5 W. The frequency graph is depicted in Figure 9, and the average frequency in the interval [380,4000] ms is 2.59 GHz.

For 30 ms-control cycles, the power graph is shown in Figure 10; the frequency-graph displays similar characteristics to that for 10 ms-control cycles depicted in Figure 9, hence not shown. The power starts at the value of 2.62 W, and after a transient period of 510 ms (or 17 control cycles), it settles in a band around 5 W. Its average in the interval [510,4000] ms is 5.0108 W, which is 0.0108 W more than the target level of 5 W. The settling time and error for BFS for the two control cycles are shown in Table III.

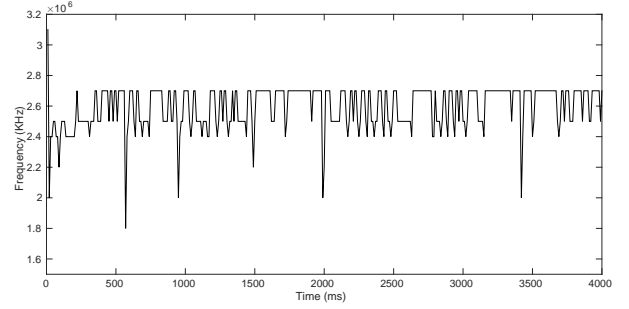


Fig. 9: BFS: clock frequency vs. time, control cycle = 10 ms

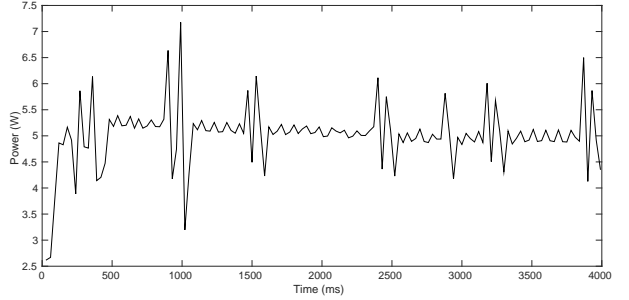


Fig. 10: BFS: power vs. time, control cycle = 30 ms

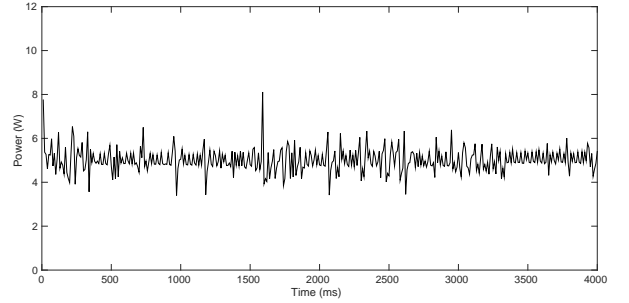


Fig. 11: KCore: power vs. time, control cycle = 10 ms

Consider next the results for Kcore. For a 10 ms-control cycle, the graphs of power and frequency vs. time are shown in Figure 11 and Figure 12, respectively. The power starts at the initial value of 7.749 W, and following an initial transient lasting 400 ms (or 40 control cycles) it settles about the target value of 5 W. The average power in the interval [400,4000] ms is 5.0124 W, which is 0.0124 W more than the target level of 5 W. The frequency graph is depicted in Figure 12, and its mean is 2.478 GHz.

For 30 ms control cycles, the power graphs are shown in Figure 13. The power starts at the value of 7.23 W, and after a transient period of 480 ms (or 16 control cycles), it settles in a band around 5 W. Its average in the interval [480,4000] ms is 5.1291 W, which is 0.1291 MIPS more than the target

TABLE III: BFS: power error and settling time

| Control Cycle (ms) | 10 | 30 |
|--------------------|--------|--------|
| Error (W) | 0.0542 | 0.0108 |
| Settling Time (ms) | 380 | 510 |

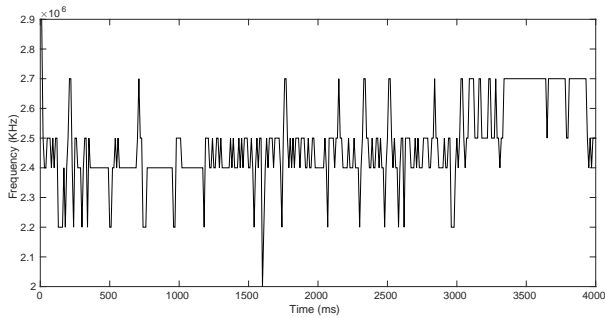


Fig. 12: KCore: clock frequency vs. time, control cycle = 10 ms

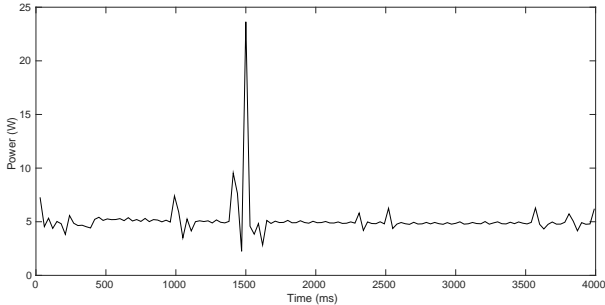


Fig. 13: KCore: power vs. time, control cycle = 30 ms

level of 5 W. The frequency graph is not shown since it is similar to the graph depicted in Figure 12 for the case of 10 ms. The average frequency is 2.608 GHz. These results are shown in Table IV.

C. Discussion and comparison of results

The entries in the four tables, namely average error and settling times, capture the performance of the regulation algorithm as applied to the four respective programs. The differences in behavior arise mainly from differences in the compute vs. memory behavior of the programs. Recall that the regulation algorithm is being applied to the operation of the cores on the processor chip - the major source of power dissipation today. The memory system is off-chip and operates in a different voltage island and off a different clock. Specifically, the processor power is directly controlled by the processor clock-rate, but only indirectly by the impact of memory instructions. Memory instructions can take two orders-of-magnitude more time to complete execution than compute instructions. Therefore the cores can stall for periods of time while waiting for memory access operations to complete. During stalls the processor consumes less power.

Further, consider the execution of a program that is memory-bound, i.e., its execution time is determined by how fast memory references can be satisfied. In this case,

running the cores in the processor at a higher speed consumes more power but produces no appreciable improvement in execution time. Conversely, a compute bound application consumes more power and takes less time when core frequency is increased. Furthermore, execution time of memory instructions can be highly variable due to congestion on the memory bus and queuing delays in the memory system. These observations help explain some of the results of the various experiments described in the previous subsections. We must point out, however, that we have a limited number of experiments for any sweeping conclusions, and those may have to wait for larger volume of data to be collected in the future.

Consider first a comparison between the two Splash-2 programs, Barnes and Ocean-nc. Barnes is compute intensive and Ocean-nc is memory intensive. Therefore we expect the power graph of Ocean-nc to display larger variability than the power graph of Barnes. That indeed can be seen by comparing the respective graphs in Figure 2 and Figure 5 for 10 ms control cycles, and in Figure 4 and Figure 7 for 30 ms control cycles. This also explains the larger settling time of Ocean-nc vs. Barnes, as can be seen in Table I and Table II. On the other hand, the tables show that the error measure for Barnes is larger than for Ocean-nc. We explain this by noting that the frequency fluctuations of Barnes are smaller than those of Ocean-nc, as expected and also shown in Figure 3 and Figure 6. If the frequency set Ω were continuous then we would expect Barnes to have the smaller error. However, the fact that Ω is a finite set suggests, by Eq. (8), that the frequency can get trapped at a particular value which leads to quantization. It is possible that the wider frequency variations of Ocean-nc makes it easier for the frequency to escape from a given value thereby reducing the quantization and resulting in smaller error.

Comparing results of the Splash-2 programs to those obtained from the GraphBig programs, the main difference is in the error measures. According to Tables I-IV, the errors for BFS and Kcore are smaller than for Barnes and Ocean-nc. Like Ocean-nc, both BFS and Kcore are also sensitive to the performance of the memory system, although for different reasons than Ocean-nc. These applications process large graphs. The ratio of compute instructions to memory instructions is smaller and the patterns of memory references are quite irregular - this makes the memory behaviors more sensitive to memory system latency. This can cause more frequent stalls by the processor cores. The regulation algorithm takes one step per control cycle and control cycles are independent of the number and duration of stalls. Therefore, on average there are less computing activities per control cycle in BFS and Kcore than in Ocean-nc; also less than Barnes which is compute intensive. This results in longer averages per frequency-variable which in turn translates into more precise computations.

Finally, we mention that for each given program there is no noticeable difference in performance between the experiments with the respective control cycles of 10 ms and 30 ms. We also note that performance of the regula-

TABLE IV: KCore: power error and settling time

| Control Cycle (ms) | 10 | 30 |
|--------------------|--------|--------|
| Error (W) | 0.0124 | 0.1291 |
| Settling Time (ms) | 400 | 480 |

tion algorithm on the GraphBig programs is quite good as indicated in Table III and Table IV, considering that these are large-scale application programs representative of data center applications.

IV. CONCLUSION

This paper describes an output-regulation technique inspired by Newton-Raphson's algorithm for solving algebraic equations. The tracking controller has the form of an integrator with adjustable gain, designed for effective regulation. The gain is adjusted in real time by simple computations in the feedback loop. Furthermore, the regulation algorithm is robust to modeling uncertainties and computing errors in the loop, hence does not require precise models of the plant.

We implemented the controller on Intel's commodity microarchitecture, Haswell, in order to test it on various industry-benchmark programs. The control variable consists of the processor's clock rate, and the controlled quantity is the spatial and temporal average of the cores' power. Due to the lack of adequate models for performance evaluation of these systems, we programmed and performed a system-identification algorithm that is executed in real time. We describe the main technical challenges associated with implementations of the controller. Results of the experiments are presented and discussed in detail, and they exhibit fast and effective convergence. To the best of our knowledge, the paper presents the first implementation of a control law at the core-level, based on formal control theory, and applied to application programs that are executed in large datacenters.

REFERENCES

- [1] X. Wang, K. Ma, and Y. Wang. Adaptive Power Control with Online Model Estimation for Chip Multiprocessors. *IEEE Transactions on Parallel and Distributed Systems*, Vol. 22, pp. 1681-1696, 2011.
- [2] P. Bohrer, N.E. Elmootazbellah, T. Keller, M. Kistler, C. Lefurgy, C. McDowell, and R. Rajamony. The casae for power management in web servers. In *Power aware computing*, pp. 261-289, Springer, USA, 2002.
- [3] P. Hammarlund, A. Martinez, A. Bajwa, D. Hill, E. Hallnor, H. Jiang, M. Dixon, M. Derr, M. Hunsaker, R. Kumar, R. Osborne, R. Rajwar, R. Singhal, R. D'Sa, R. Chappell, S. Kaushik, S. Chennupati, S. Jourdan, S. Gunther, T. Piazza, and T. Butron. Haswell: The Fourth-Generation Intel Core Processor. *Micro*, Volume 34, pp. 6-20, 2014.
- [4] K. Skadron, M. R. Stan, W. Huang, S. Velusamy, K. Sankaranarayanan, and D. Tarjan. Temperature-aware microarchitecture. *ACM SIGARCH Computer Architecture*, Vol. 31, pp. 213, 2003.
- [5] G. Liu, M. Fan, and G. Quan. Neighbor-aware dynamic thermal management for multi-core platform. *Design, Automation and Test in Europe Conference and Exhibition*, Dresden, Germany, March 12-16, 2012.
- [6] I. Yeo, C.C. Liu, and E.J. Kim. Predictive dynamic thermal management for multicore systems. *Design Automation Conference*, Anaheim, CA, USA, June 8-13, 2008.
- [7] S.W. Kim, T.M. Kim and C. Yoo. Workload prediction using run-length encoding for runtime processor power management. *Electronics Letters*, Vol. 51, pp. 1759-1761, 2015.
- [8] N. Avirneni, P. Ramesh, and A. Soman. Utilization Aware Power Management in Reliable and Aggressive Chip Multi Processors. *IEEE TRANSACTIONS ON COMPUTERS*, Volume 65, pp. 979-991, 2016.
- [9] R. Raghavendra, P. Ranganathan, V. Talwar, Z. Wang, and X. Zhu. No power struggles: coordinated multi-level power management for the data center. *SIGARCH Comput. Architecture News*, Volume 36, pp. 48-59, 2008.
- [10] A. Mishra, S. Srikantiah, M. Kandemir, and C. Das. Cpm in cmps: Coordinated power management in chip-multiprocessors. *Intl. Conference on High Performance Computing, Networking, Storage and Analysis*, New Orleans, LA, USA, Nov. 13-19, 2010.
- [11] J.L. Hellerstein, Y. Diao, S. Parekh, and D.M. Tilbury. *Feedback Control of Computing Systems*, John Wiley & Sons, 2004.
- [12] A. Deval, A. Ananthakrishnan, and C. Forbell. Power management on 14 nm Intel Core M processor. *Low-Power and High-Speed Chips*, Yokohama, Japan, April 13-15, 2015.
- [13] V. Krishnaswamy, J. Brooks, G. Konstantinidis, C. McAllister, H. Pham, S. Turullols, J. Shin, Y. Gong, and H. Zhang. Fine-Grained Adaptive Power Management of the SPARC M7 Processor. *Solid-State Circuits Conference*, San Francisco, CA, Feb 22-26, 2015.
- [14] H. Chen, A. Coskun, and M. Caramanis. Real-Time Power Control of Data Centers for Providing Regulation Service. *IEEE Conference on Decision and Control*, Florence, Italy, Dec 10-13, 2013.
- [15] C. Lefurgy, X. Wang, and M. Ware. Power Capping: a Prelude to Power Shifting. *Cluster Computing*, Volume 11, pp. 183 to 195, 2008.
- [16] G.F. Franklin, J.D. Powell, and A. Emami-Naeini. *Feedback Control of Dynamic Systems*, Prentice Hall, Pearson, 2014.
- [17] N. Almoosa, W. Song, S. Yalamanchili, and Y. Wardi. A Power Capping Controller for Multicore Processors. *Proc. American Control Conference*, Montreal, Canada, June 27-29, 2012.
- [18] Y. Wardi, C. Seatzu, X. Chen, and S. Yalamanchili. Performance Regulation of Stochastic Discrete Event Dynamic Systems Using Infinitesimal Perturbation Analysis. *Nonlinear Analysis: Hybrid Systems*, Volume 22, pp.116-136, November 2016.
- [19] N. Almoosa, W. Song, Y. Wardi, and S. Yalamanchili. Throughput Regulation in Multicore Processors via IPA. *Proc. 51 IEEE Conference on Decision and Control (CDC)*, Maui, Hawaii, December 10-13.
- [20] X. Chen, H. Xiao, Y. Wardi, and S. Yalamanchili. Throughput Regulation in Shared Memory Multicore Processors. *IEEE International Conference on High Performance Computing*, Bangalore, India, December 2015.
- [21] C. Seatzu and Y. Wardi. Performance Regulation Via Integral Control in a Class of Stochastic Discrete Event Dynamic Systems. *Proc. 12th International Workshop on Discrete Event Systems, WODES 2014*, Cachan, France, May 14-16, 2014.
- [22] X. Chen, Y. Wardi, and S. Yalamanchili. IPA in the Loop: Control Design for Throughput Regulation in Computer Processors. *Proc. 13th Intl. Workshop on Discrete Event Systems (WODES'16)*, Xi'an, China, May 30 to June 1, 2016.
- [23] P. Lancaster. Error analysis for the Newton-Raphson method. *Numerische Mathematik*, Vol. 9, pp. 55-68, 1966.
- [24] Y.C. Ho and X.R. Cao. *Perturbation Analysis of Discrete Event Dynamic Systems*, Kluwer Academic Publishers, Boston, Massachusetts, 1991.
- [25] C.G. Cassandras and S. Lafortune. *Introduction to Discrete Event Systems*, Springer Science+Business Media, New York, 2008.
- [26] J.L. Hennessy and D.A. Patterson. *Computer Architecture: A Quantitative Approach*, Morgan Kaufmann, 2012.
- [27] K. Keesman. *System identification: an introduction*. Springer Science & Business Media, 2011.
- [28] S.C. Woo, M. Oharat, E. Torriet, J. Singhi, and A. Gupta. The SPLASH-2 Programs: Characterization and Methodological Considerations. *Proc. 22nd Annual International Symposium on Computer architectures*, pp. 24-36, S. Margherita Ligure, Italy, June 22-24, 2005.
- [29] L. Nai, Y. Xia, I. Tanase, H. Kimy, and C. Lin. GraphBIG: Understanding Graph Computing in the Context of Industrial Solutions. *International Conference for High Performance Computing, Networking, Storage and Analysis*, Austin, TX, Nov. 15-20, 2015.
- [30] S. Browne, J. Dongarra, N. Garner, G. Ho, and P. Mucci. A Portable Programming Interface for Performance Evaluation on Modern Processors. *The International Journal of High Performance Computing Applications*, Volume 14, number 3, pp. 189-204, Fall 2000.